IMPLOSION SOURCE DEVELOPMENT AND DIEGO GARCIA REFLECTIONS

Philip E. Harben and Carl O. Boro
Lawrence Livermore National Laboratory

Sponsored by
National Nuclear Security Administration
Office of Nonproliferation Research and Engineering
Office of Defense Nuclear Nonproliferation

Contract No. W-7405-ENG-48

ABSTRACT

Calibration of hydroacoustic stations for nuclear explosion monitoring is important for increasing monitoring capability and confidence from newly installed stations and from existing stations. Past work at Ascension Island has shown that ship-towed airguns can be effectively used for local calibrations such as sensor location, amplitude and phase response, and T-phase coupling in the case of T-phase stations. At regional and ocean-basin distances from a station, the calibration focus is on acoustic travel time, transmission loss, bathymetric shadowing, diffraction, and reflection as recorded at a particular station. Such station calibrations will lead to an overall network calibration that seeks to maximize detection, location, and discrimination capability of events with acoustic signatures.

Active-source calibration of hydroacoustic stations at regional and ocean-basin scales has not been attempted to date, but we have made significant headway addressing how such calibrations could be accomplished. We have developed an imploding sphere source that can be used instead of explosives on research and commercial vessels without restriction. The imploding sphere has been modeled using the Lawrence Livermore National Laboratory hydrodynamic code CALE and shown to agree with field data. The need for boosted energy in the monitoring band (2-100 Hz) has led us to develop a 5-sphere implosion device that was tested in the Pacific Ocean earlier this year. Boosting the energy in the monitoring band can be accomplished by a combination of increasing the implosion volume (i.e. the 5-sphere device) and imploding at shallower depths.

Although active source calibrations will be necessary at particular locations and for particular objectives, the newly installed Diego Garcia station in the Indian Ocean has shown that earthquakes can be used to help understand regional blockages and the locations responsible for observed hydroacoustic reflections. We have analyzed several events with a back azimuth from Diego Garcia between 100 and 140 degrees. The Diego Garcia records show a pronounced reflection that correlates in travel time and back azimuth (calculated using the waveform cross-correlation of the tri-partite array elements to determine lag time across the array) with a reflector at the Saya de Malha Bank, on the Seychelles-Mauritius Plateau. We also show that to accurately predict blockage and reflection regions, it is essential to have detailed bathymetry in relatively small but critical areas.

KEY WORDS: calibration, hydroacoustic

OBJECTIVE

Results from the Ascension Island experiment show that for a local hydroacoustic station calibration, an airgun array can accomplish a number of calibration objectives:

1. Accurate location of sensors using numerous precise shot locations (Harben, 1999).
2. Amplitude and phase calibration of the sensors based on good source repeatability (Harben, 2000).
3. Acoustic-to-seismic coupling calibration in the case of T-phase stations (Rodgers, 2000).

Although local station calibrations are necessary to understand the response of a given station, they are not sufficient to understand and characterize the hydroacoustic network performance. Ideally, ocean-basin scale network calibrations with controlled sources would give the network capability assurance that is ultimately desired. Toward this end we have been investigating two issues that have bearing on full network capability assessments. These issues are: long-range acoustic sources for active calibrations and ground truth and reflections and the use of reflected data in network capability assessment. We first present work accomplished on an imploding glass sphere source with the objective of producing an effective long-distance in-band SOFAR (Sound Fixing and Ranging) axis source free from the safety hazards of explosives. Next we present an example of a specific acoustic reflection observed for several earthquakes recorded at Diego Garcia, assessing the back azimuth estimation capabilities of the tri-partite arrays and suggesting how these reflections may be used to improve hydroacoustic monitoring capabilities.

RESEARCH ACCOMPLISHED

The two calibration topics discussed are *implosion source development* and *Diego Garcia reflections*. It should be noted that these studies have their place in a future ocean-basin scale network calibration, the former being one potential source of a number of possibilities that have yet to be tested, the latter being quantified and optimized to improve network detection and location accuracy.

Implosion Source Development

The implosion concept and prototype-controlled imploder have been discussed in a previous paper (Harben et al, 2000). Briefly, an implosive acoustic source is desirable because it offers the potential for SOFAR-depth sources with the acoustic energy release of a small explosion (nominally 1-5 pounds equivalent) but without any of the hazards of explosives. A controlled implosion system developed at Lawrence Livermore National Laboratory (LLNL) uses a cylinder and piston-ram assembly affixed to a 22-liter glass sphere. One end of the cylinder is capped with a pressure-calibrated rupture disc. The other end of the cylinder faces the glass sphere with an external ram attached to the internal piston. When the rupture disc fails, the in-rush of high-pressure seawater drives the piston and external ram into the sphere with sufficient force to shatter it and initiate the implosion.

Implosion results from earlier studies and presented in last year's symposium proceedings (Pulli et. al., 2000) have shown that a 22-liter sphere imploded at a nominal SOFAR channel depth (700 meters) results in a fairly high-frequency acoustic pulse, with the bulk of the acoustic energy out of the monitoring band (2-100 Hz). Two methods that will tend to enhance energy at lower frequencies are: 1) to implode at a shallower depth and 2) to implode a larger sphere volume. Imploding at a shallower depth has the drawbacks of producing a less energetic acoustic pulse due to the lower implosion pressures at shallower depths and producing less efficient coupling of the energy into the SOFAR channel due to the unfavorable ray geometry for trapping energy in the SOFAR channel. A larger implosion source has cost and design implications that require modifying the implosion system. We have looked at both these methods and conducted a field test to determine if we can pump more energy into the frequency band of monitoring interest.

Imploding at a shallower depth was tested using the same single-sphere system used in a test conducted last year. The depth of implosion was 340 meters, half the depth of the previous test. The waveforms of the two tests are shown in Figure 1. Both tests show the characteristic waveform of an imploding sphere: an initial rarefaction pulse during the implosion/compression stage of the collapse followed by a very sharp pressure spike at the instant of complete collapse and motion reversal. A small bubble pulse is also evident. In comparing the two time histories, it is evident that the shallower test had a lower peak pressure, longer collapse time and a longer bubble pulse period. The bubble pulse oscillations from an implosion are analogous to the oscillations from an explosion; however, the details of the physics are quite different. Qualitatively, an explosion generates a shock wave as the explosive rapidly burns and expands. The gas globe consisting of the explosion products expands beyond the diameter of equilibrium pressure with the

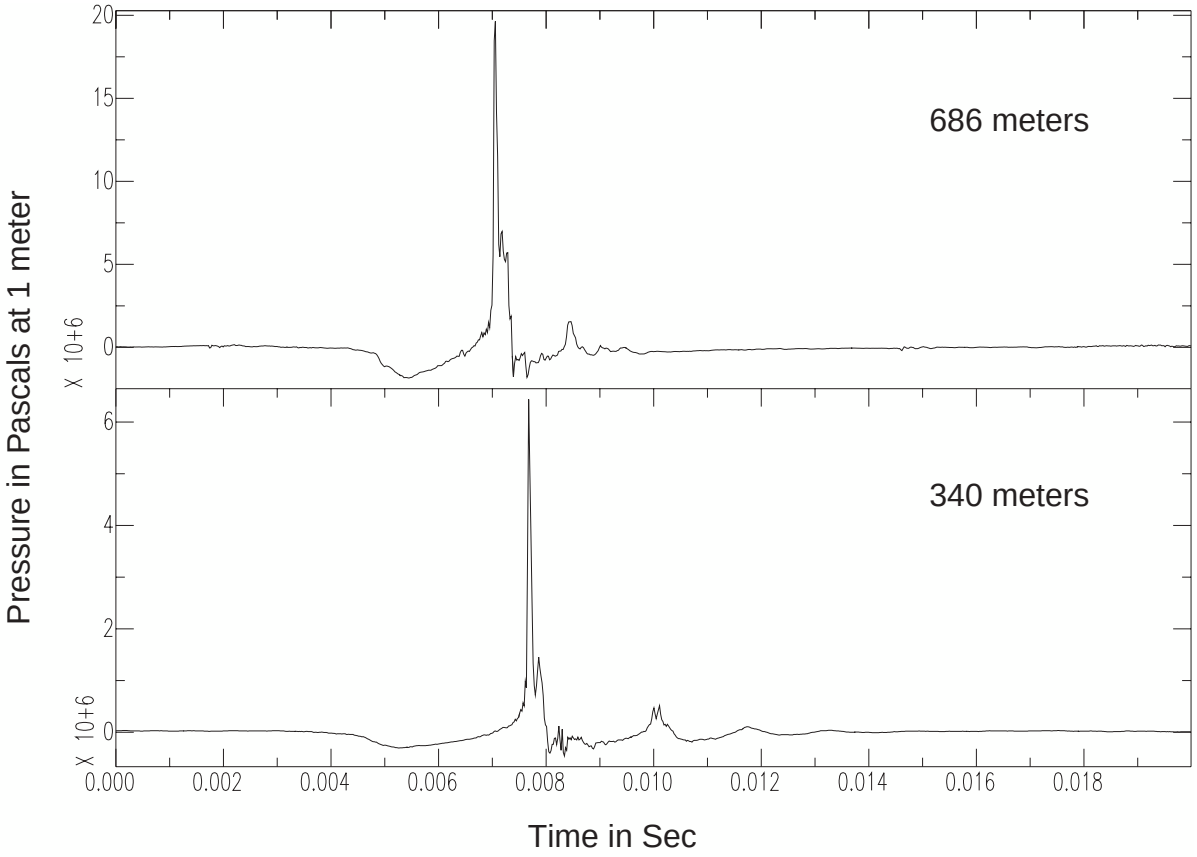

Figure 1. The recorded waveforms from two single-sphere implosion tests. The top test was conducted at 686-meters depth, the bottom at 340-meters depth. Recording is by a ship-suspended hydrophone at nominally 12-meters depth.

ambient seawater then contracts, to oscillate about the equilibrium globe size, giving a bubble pulse at each instant of expansion from a minimum globe size. The implosion begins with a rarefactional pulse as the sphere collapses then generates a shock wave at minimum sphere volume, expanding to oscillate about the ambient pressure. The imploding sphere, however, has a very low gas density relative to the explosion and hence bubble pulses are not pronounced or persistent. The measured values for collapse time, bubble pulse period, and peak pressure are shown in Table 1 below. The values in the table also show results for a single-sphere implosion at 130 meters. This was taken from the initial record of the 5-sphere collapse shown in Figure 3.

	686 meters	**340 meters**	**130 meters**
Peak Pressure (Pa)	2.0×10^7	6.5×10^6	5.0×10^5
Collapse Time (msec)	2.7	4.4	6.9
Bubble Pulse Period (msec)	1.3	2.4	----

Table 1. Measured Values for Implosion Experiment

The bubble pulse period has been shown for explosions to be inversely proportional to (see Urick, 1983) $d^{5/6}$ for depth, d, greater than 100 meters. This is consistent with the observed bubble pulse period differences between 686 meters and 340 meters. A bubble pulse period could not be determined for the 130-meter test because of the interference created by the collapse of the other four spheres.

The pressure peak and collapse time were calculated using the LLNL hydrodynamics code CALE (see Tipton, 1991) by Clark, 2001, for the 686-meter case and found reasonable agreement in peak pressure (1.18×10^7 Pa calculated vs 2.0×10^7 Pa actual) and collapse time (2.0 msec calculated vs 2.7 msec actual). As of this writing, model predictions of peak pressure and collapse time at other depths have not been conducted. It should be noted that implosion collapse modeling of the acoustic frequency spectrum has been conducted by Guerin et al, 2001. Because we could not record at a high enough sample rate on the ocean bottom hydrophone, we cannot compare our results directly to these models.

Increasing the implosion volume by increasing the diameter of the implosion sphere is impractical from a cost and operational standpoint. The 22-liter spheres we used are about the largest we have found commercially. To produce a significantly larger sphere would require special development and substantially thicker walls. Such a sphere would be costly, heavy, and large. We chose instead to cluster a number of the spheres together and thereby increase the overall volume of the implosion. A photograph of the prototype device is shown in Figure 2. The device consists of orthogonal steel planar forms that serve to hold the spheres in place, the same smashing cylinder as used in the single sphere system, and the five spheres. The idea is simple: smash one sphere and the rest will shatter in sympathy once the shock wave from the first implosion develops.

Figure 2. The prototype 5-sphere implosion system is shown next to the 1-sphere system. The smashing cylinder is the same for both.

We tested the 5-sphere system at 130-meters depth. The implosion test was about as large and as shallow as deemed likely in any hydroacoustic monitoring calibration scenario that would use such sources and hence shows about the best that can be easily achieved in pumping more relative acoustic energy into the monitoring frequency band. The 5-sphere implosion waveform, shown in Figure 3, was recorded at a sample rate of 16 kHz on the near-surface hydrophone, fast enough to capture many details of the implosion.

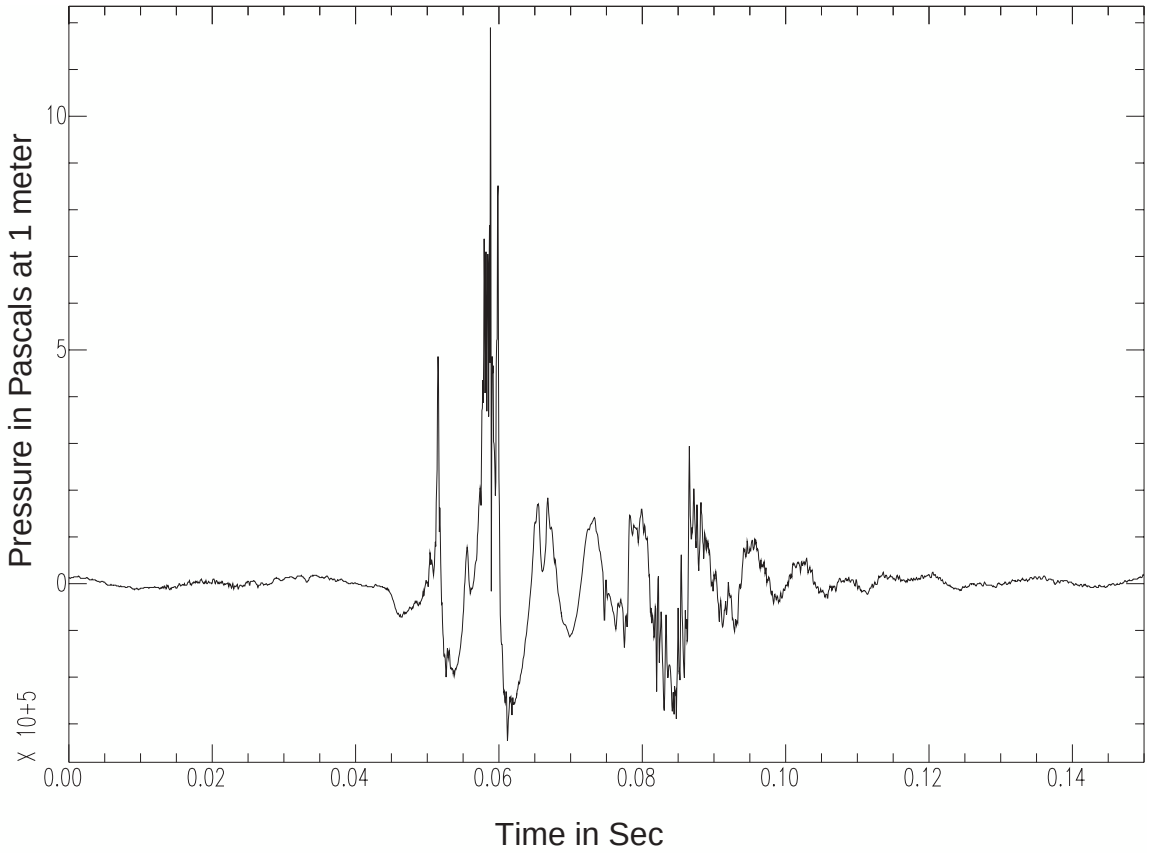

Figure 3. The recorded waveform for the 5-sphere implosion conducted at 13-meters depth. Recording is by a ship-suspended hydrophone at 12 meters nominal depth.

The characteristic collapse of a single sphere is seen in the beginning of the record. The peak pressure and collapse time from this were used to fill in the 130-meter column within the table above. After the peak pressure spike from the first imploding sphere, a larger collapse event is evident followed by a complex pressure spike. We believe this to be the nearly simultaneous collapse and peak pressure spikes from the other four spheres. A complex bubble pulse interference follows with high-frequency hash arriving at about 0.08 sec, consistent with a reflection of the acoustic energy from the free surface.

Unfortunately, the near surface hydrophone recording is not a quantitative indicator of the low-frequency content in the acoustic signal because of interference from the reflection off the ocean surface. It is best to record the signal as deep as possible. This was done during the recent series of sea tests by deploying several Ocean Bottom Seismometers (OBS) with associated hydrophones. Although the hydrophone record obtained at 1.2-km depth was only sampled at 125 Hz with an anti-alias filter at 33 Hz, the 5-sphere recording showed over 80 Db S/N in the acoustic energy density between 3 and 33 Hz. Based on cylindrical spreading in the sound channel and the very low attenuation at these low frequencies, this signal level coupled in the sound channel should be observable thousands of kilometers from the source. What we have failed to determine in these tests is how effectively we couple signal into the sound channel and how this coupling changes as the depth of the source is varied. To conduct these experiment we will need

hydrophones in the SOFAR channel at large distances from the source. Upcoming experiments will allow us to make these measurements.

Diego Garcia Reflections

The observation of hydroacoustic reflections off topographic features is not new (see Kibblewhite et al, 1969 and Northrop, 1968). A recent study by Pulli et al, 2000, has revisited some historical explosions that exhibit topographic reflections and concluded that there is a potential for using reflections to enhance hydroacoustic monitoring capabilities. Since this study, the Diego Garcia (DG) station has come on-line. The north arm of the new Diego Garcia (DGnorth) station was operational by the middle of 2000 and the south arm (DGsouth) of the station near the end of 2000. This is the first International Monitoring System hydroacoustic station that conforms to specifications and has been certified. Many research teams are now examining this new data set and are finding interesting things that will be reported elsewhere. Of particular interest in this study is the potential for using the tri-partite arrangement of hydrophones to calculate a back azimuth and thereby provide an automated method to associate and pinpoint reflected phases. We examined four large (greater than M 4.5) oceanic earthquakes that vary in bearing from about 100 degrees from DG to about 140 degrees (see Figure 4). Three of the four earthquakes occurred before DGsouth was on-line. We analyzed the T-phases recorded by the station to see if accurate back azimuths could be determined and to determine if arrivals after the direct T-phase could be reflections of the direct phase off some bathymetric obstacle.

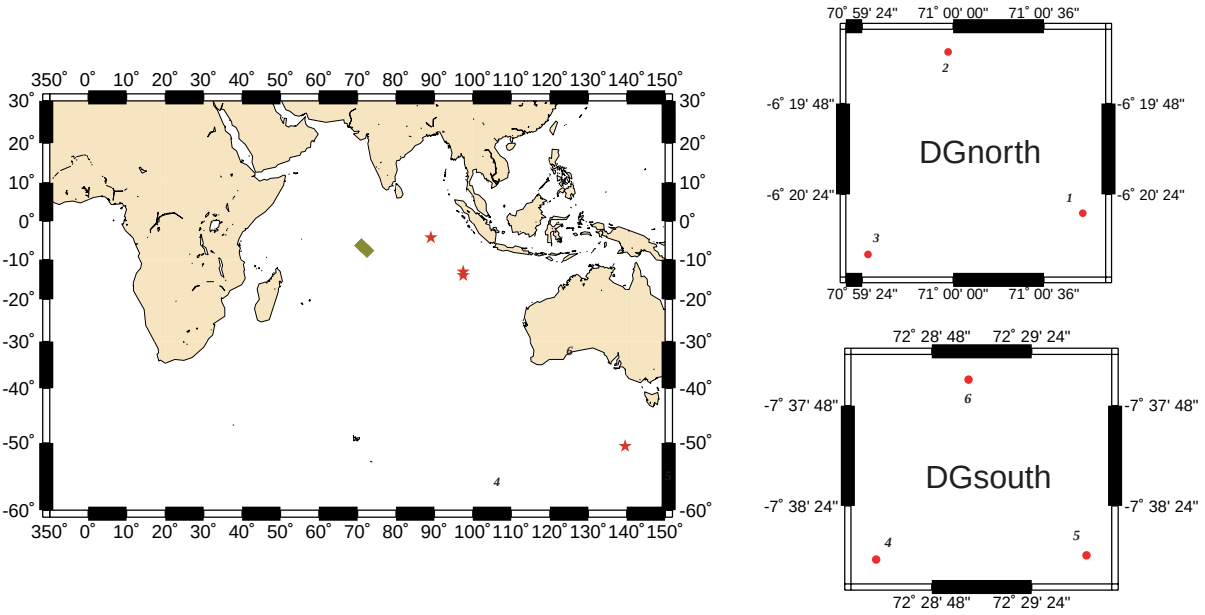

Figure 4. The left map shows the four earthquakes analyzed (stars) and the two Diego Garcia station arms (diamonds). The right maps show the sensor layout for the north (top) and south (bottom) arms of the station.

The spacing of the north-arm hydrophones is about 2.5 km, too large to use standard array processing given that the nominal frequency band of these earthquake generated T-phase signals is 2-12 Hz. Instead, we assumed a coherent plane wave and looked for the lags in the peaks of the signal cross-correlations among sensor elements. We used a 40-second time window that encompassed the bulk of the signal. The windowed waveforms were band-passed with lower and upper corners of 2 Hz and 12 Hz, respectively. These signals were then cross-correlated to determine the lag in the cross-correlation peaks and derive a back azimuth. The same process was applied to all the direct and reflected phases discussed herein. The process is shown in Figure 5 for both the direct phase and a specific reflected phase of a June 18, 2000, Mb 6.8 earthquake located in the South Indian Ocean (the nearly over-plotted stars in the Figure 4 map). This earthquake was about 3010 km from DGnorth on a bearing of 108 degrees from the station. The lags in the cross-correlation peaks of the direct T-phase (the left plot on Figure 5) give a back azimuth of 111 degrees, only

3 degrees from the true value. Notice the relatively poor S/N of the cross-correlation peaks as compared to those from the reflected phase (the right plot in Figure 5) even though the S/N of the direct phase is much larger that the reflected phase. We will discuss the likely cause for this observation at the end of this section. The bearing from DGnorth to the

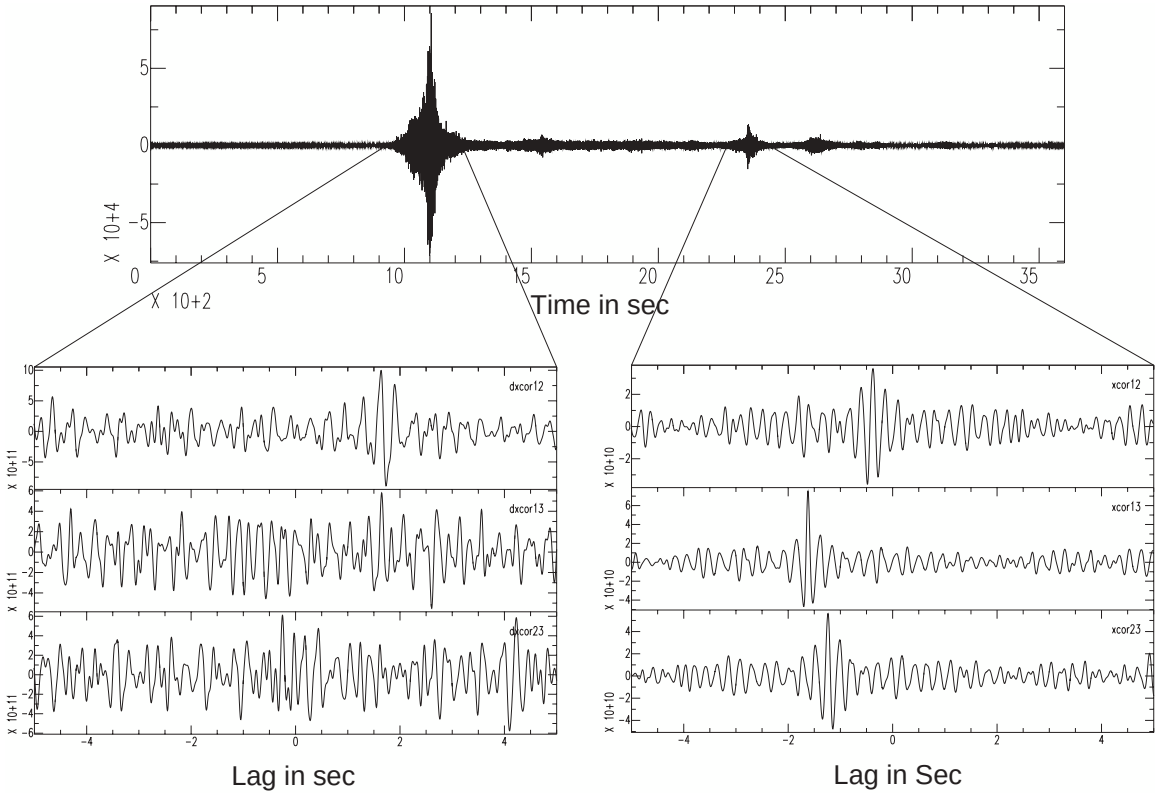

Figure 5. The 6/18/2000 M 6.8 Indian Ocean earthquake is shown at top as recorded by DG01. The waveform cross-correlations of the three north-arm elements are shown for the windows indicated. Notice the direct T-phase (left) has relatively poor cross-correlation peaks compared to a reflected phase (right) despite the much larger S/N of the direct phase.

reflection source as determined by the lags in the cross-correlation peaks is 246 degrees. If we plot the paths of the direct T-phase from the earthquake to DGnorth and the path 246 degrees from DGnorth to the nearest possible bathymetric reflector, we get the presumed reflected T-phase path as shown in Figure 6. The arrival time of such a reflected path is consistent with the observed arrival time, and spectrograms of both the direct and reflected phase are remarkably similar in frequency content and duration. We conclude that the Saya de Malha Bank of the Seychelles-Mauritius Plateau is the likely T-phase reflector for this earthquake.

We analyzed a number of other phases arriving after the direct T-phases for the earthquakes shown in Figure 4. Some gave the same back azimuth as the direct T-phase and consequently may have been aftershocks. Others gave different bearings. We will only focus on the one particular reflection source determined in Figure 5 and Figure 6, the Saya de Malha Bank, and see if other earthquakes on similar bearings produce an observable reflection off the same reflector.

A South Indian earthquake on 9/17/2000, shown nearly over-plotted with the 6/18/2000 event in Figure 4, is a Mb 4.7 presumed aftershock. Although the ratio of signal to noise (S/N) of the direct phase from this event is high, we could not determine a back azimuth because of poor correlation among the tri-partite hydrophones. A phase barely above the noise with arrival time consistent with the same reflection path of Figure 6 was analyzed and found to have surprisingly high correlation among the tri-partite hydrophones with good agreement for the cross-correlation peaks. The back azimuth was 246 degrees, consistent with a reflection off the Saya de Malha Bank.

Finally, an Mb 5.9 earthquake from the West Indian Ocean/Antarctic Ridge (lowest right in Figure 4) on June 11, 2000, was analyzed in the same way as the previous events. The back azimuth of the direct T-phase was calculated from the array elements to be 141 degrees compared to an actual back azimuth of 141 degrees. A reflected phase with poor S/N was identified on the time history recordings with an arrival time consistent with a reflection off the Saya de Malha Bank on the Seychelles/Mauritius Plateau. The back azimuth calculated with the tri-partite hydrophones for this phase had a bearing of 244 degrees, consistent with a reflection off the Bank. We conclude that for this event a reflection off the Saya de Malha Bank is observed. It should be noted that, as in the previous events, the S/N of the peak in the cross-correlation function was also far higher for the low-S/N reflected signal than for the high-S/N direct T-phase.

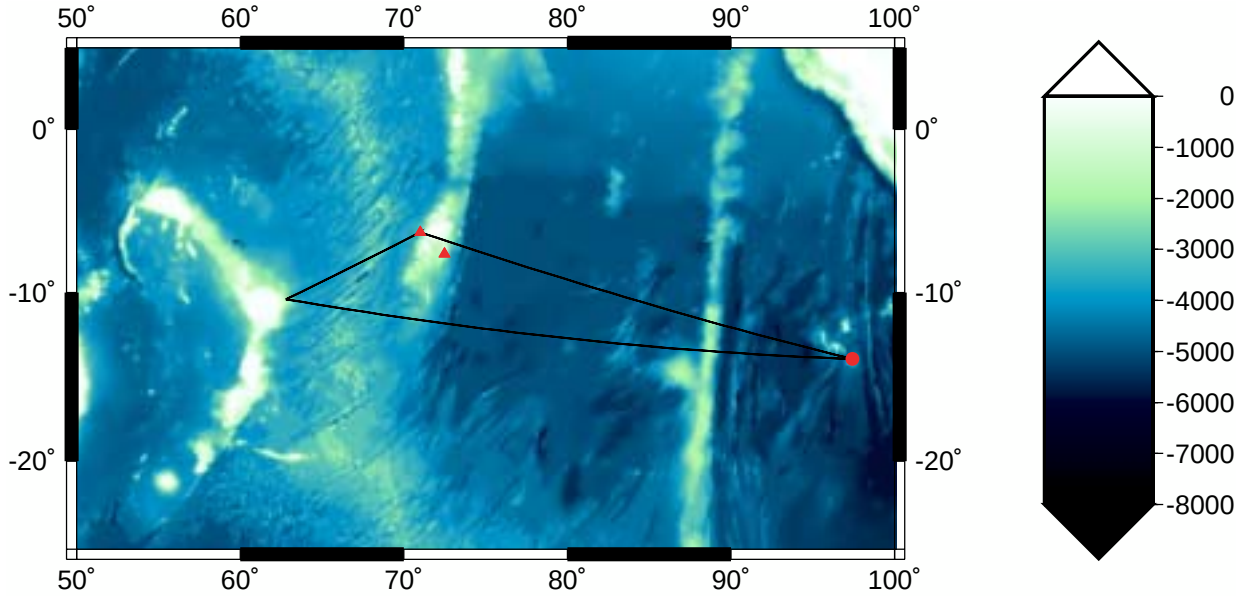

Figure 6. The regional bathymetry with the Diego Station arms (triangles) with the direct and reflected path from the 6/16/2000 earthquake (circle) to the north arm of the Diego Garcia station.

The reason for the poor S/N of the direct T-phase cross-correlation peaks when compared to the reflected cross-correlations is probably due to local Diego Garcia bathymetric scattering of the plane wave along the direct path. The scattering presumably results in poor spatial coherence of the signal when it reaches the sensors, even though the S/N is still quite large. No such bathymetric obstacle (other than the reflector) exists on the reflected path. This does not rule out the possibility that the modal composition of the direct T-phase is changed upon reflection to produce a more spatially coherent signal. A recent event (Mb 4.9 on 3/11/2001, after the south arm of DG became operational, the northernmost on the map of Figure 4) pretty much rules out modal composition change as the main reason for the observed S/N differences of the sensor cross-correlation peaks. That event had poor S/N for cross-correlation peaks of the direct T-phase signal at the north arm but excellent S/N of the cross-correlation peaks of the direct T-phase at the south arm where there were no bathymetric obstacles along the path. If complex modal composition of the direct T-phase was the cause of poor S/N of the cross-correlation peaks, then we would expect it on both the north and south arms.

CONCLUSIONS AND RECOMMENDATIONS

A large-scale calibration experiment that tests a number of sources against the various calibration objectives is a first step in defining what an ocean-basin-scale calibration of the hydroacoustic monitoring network will consist of. It is clear at the outset that no one source will accomplish all of our objectives. Implosion sources, airguns, explosions, and other sources will be tested during the next two years to determine the range scale and calibration objective each is suited for. Our recent work on implosion sources indicates that we can boost energy in the monitoring frequency band and that such a source may be useful for inexpensively and safely gathering travel-time, transmission loss, and

blockage calibration data on a regional to ocean-basin scale. Tests will soon be conducted in the Indian Ocean that will determine just what range-scale the implosion source will be applicable to. One point is clear: the implosion source is far too small to be used for any type of reflection calibration. Such calibrations will have to use special purpose low-frequency sources or fairly large explosions.

Data from the Diego Garcia station --with the tri-partite sensor arrays-- have been full of surprises that beg a rethinking of just how to process hydroacoustic data in a monitoring context and how far we can go in squeezing more capability out of a sparse sensor network. We have documented that consistent reflections occur for sources at particular bearings from the station. In addition, we showed that fairly accurate (within a few degrees) back azimuth estimates of the direct and reflected signal could be determined by examining broadband cross-correlations of the signals across the array elements. Using active sources and natural events, a database of the reflection zones in the Indian Ocean can be developed. If the reflection zones can be sufficiently localized, reflected phases may be able to enhance network location capability. At the very least, reflected phases may be the only path that reaches a particular station arm that is otherwise blocked by topography and hence the only way for that particular station to be used in a detection, location, or discrimination scheme.

ACKNOWLEDGEMENTS

We thank Leroy Dorman and Allen Sauter of the Scripps Institution of Oceanography for support during the field test aboard the R.V. Sproul, provided by the National Science Foundation under grant OCE 97-12605. Doug Clarke provided the CALE simulation of the implosion. Richard Baumstark of the Air Force Technical Applications Center supplied the Diego Garcia recordings.

REFERENCES

Guerin, J-M and P-F Piserchia (2001), Analysis of the Hydro-acoustic Energy Released by an Implosion of a Glass Sphere, Commissariat a l Energie Atomique, DAM DIF DASE.

Hanson, J.A. and P.E. Harben (2000), Acoustic-to-Seismic Wave Coupling Study at Ascension Island, Proc. SSA Annual Mtg., April, 2000.

Harben, P.E., J.R. Hollfelder, and A.J. Rodgers (1999), Experimentally Determined Coordinates for Three MILS Hydrophones near Ascension Island, UCRL-ID-136507.

Harben, P.E., D.K. Blackman, A.J. Rodgers, C. Turpin, and J.R. Hollfelder (2000), Calibration Factors for Three MILS Hydrophones Near Ascension Island, UCRL-ID-138036.

Harben, P.E., C. Boro, L. Dorman, and J. Pulli (2000), Use of Imploding Spheres: An Alternative to Explosives As Acoustic Sources At Mid-Latitude SOFAR Channel Depths, UCRL-ID-139032.

Kibblewhite, A.C. and R.N. Denham (1969), Hydroacoustic Signals from the Chase V Explosion, J. Acoust. Soc. Am., 45, 944-956.

Northrop, J. (1968), SubmarineTopographic Echos from Chase V, J. Geophys. Res., 73, 3909-3916.

Pulli, J.J., Z. Upton, R. Gibson, J. Angell, T. Farrell, and R. Nadel (2000), Characterization of Reflected Arrivals and Implications for Hydroacoustic Test-Ban-Treaty Monitoring, BBN Tech. Memor. W1380.

Pulli J.J. and P.E. Harben (2000), Hydroacoustic Calibration with Imploding Glass Spheres, in 22nd Annual DoD/DOE Seismic Research Proc., Vol. III, pp. 65-74.

Tipton, R. (1991), CALE User s Manual, Version 920701, Lawrence Livermore National Laboratory, Livermore, CA.

Urick, R.J. (1983), Principles of Underwater Sound, Peninsula Publishing, Los Altos, CA.